

Chirping in Plasmas: test of criterion for onset and simulation of explosive chirping

H.L. Berk¹, B.N. Breizman¹, V.N. Duarte², N.N. Gorelenkov³, W. W. Heidbrink⁴, G. Kramer³, N. Nazikian³, D.C. Pace⁵, M. Podesta³, B.J. Tobias³, M.A. Van Zeeland⁵, G. Wang¹ and L. Zheng¹

¹University of Texas at Austin, Austin, TX, 78723, USA

²Institute of Physics, University of Sao Paulo, Sao Paulo, SP, 05508-090, Brazil

³Princeton Plasma Physics Laboratory, Princeton, NJ, 08543, USA

⁴University of California Irvine; Irvine, CA, 92697, USA

⁵General Atomics, San Diego, CA, 92186, USA

Corresponding Author: hberk@mail.utexas.edu

Abstract:

Two extreme scenarios for frequency sweeping of Alfvénic oscillation is studied. First we use the generalized form of a criterion found by Lilley et.al. [1] that assesses whether marginally unstable Alfvénic modes destabilized by energetic particles (EPs) are either likely to chirp or to remain as steady. This criterion is applied to NSTX and DIII-D data to predict whether chirping or steady Alfvénic oscillations are likely. Chirping arises in DIII-D when background turbulence markedly decreases. The second investigation examines the plasma response from an energetic particle source that increases in time. Instabilities are found for the TAE, with a limited range chirping, and EPM, with a fast and extended chirping range, by employing a new simulation technique that enables a significantly increased time-step to be used. The results of the simulations is explained from analytic theory that shows a fast chirping that is still slow enough for validity of adiabatic theory.

1 Part I. Chirp criterion applied to NSTX; DIII-D

The criterion, for whether chirping or steady oscillations arise is related to whether stochastic diffusive or drag processes dominate the nonlinear response of energetic particles near marginal instability. Stochasticity promotes steady behavior, while drag promotes chirping. The equation that needs to be analyzed is an extension of a time delayed cubic equation in the mode amplitude which describes the dynamics of a system close to marginal stability, where stochastic processes acting on the resonant particles, such as pitch angle scattering, lead to diffusive relaxation processes which can prevent distribution steepening caused by nonlinear wave motion and produce a steady nonlinear wave whose amplitude is proportional to an increment above the marginal stability state of the system as was derived in Refs.[9, 11]. However, if the stochastic processes are too

small, these steady solutions are unstable and the cubic equation predicts an explosive solution, where the relaxation processes are no longer important and nonlinear steepening is enabled, leading to a solution of the cubic equation where the mode amplitude diverges in a finite time. This divergence is indicative of the breakdown of validity of the cubic equation. More accurate numerical simulation [10] shows that the explosive solution is a precursor to the development of a frequency chirping response caused by the formation of phase space holes or clumps.

In Ref.[1], the drag term was added to the kinetic equation for the resonant energetic particles, to obtain a kinetic equation, which takes the normalized form,

$$\frac{\partial f}{\partial t} + \Omega \frac{\partial f}{\partial \theta} - \nu_{drag}^2 \frac{\partial f}{\partial \Omega} - \nu_{stoch}^3 \frac{\partial^2 f}{\partial \Omega^2} - \omega_b^2 \sin(\theta - \omega t) \frac{\partial f}{\partial \Omega} = 0. \quad (1)$$

Here θ is the resonant particle's angle coordinate that is conjugate to the particle's action, $\Omega = d\theta/dt$, and ω_b^2 is proportional to the mode amplitude, $A(t)$ (physically ω_b is the trapping frequency of a particle deeply trapped in the wave), ν_{stoch}^3 is the normalized diffusion of the resonant energetic particle arising from stochastic processes such as pitch angle scattering and ν_{drag}^2 is the normalized drag. Solving this equation together with the wave equation for the system, leads to the time delayed cubic equation,

$$\frac{dA}{dt} - A = - \int_0^{t/2} d\tau \tau^2 A(t - \tau) \int_0^{t-2\tau} d\tau_1 e^{-\nu_{stoch}^3 \tau^2 (2\tau/3 + \tau_1) + \nu_{drag}^2 \tau (\tau + \tau_1)} \cdot A(t - \tau - \tau_1) A^*(t - 2\tau - \tau_1). \quad (2)$$

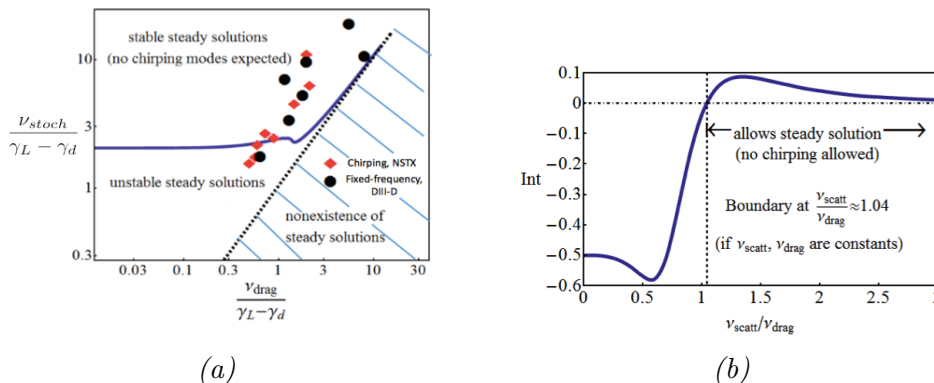
An analysis of the solutions of this equation was made in Ref [1], which produced Fig.(1a), that shows as a function of ν_{stoch}/ν_{drag} that there are regions where steady solutions are: (A) stable, (to the left and above the solid curve); (B) unstable (below the solid curve and above dotted line) and (C) did not exist (the hatched region of the figure). The non-existence condition for a steady solution is given by,

$$Crt = Int(E, P_\phi, \mu) \equiv \Re \int_0^\infty dz \frac{z}{\frac{\nu_{stoch}^3}{\nu_{drag}^3} - \imath} \exp \left[-\frac{2}{3} \frac{\nu_{stoch}^3}{\nu_{drag}^3} z^3 + \imath z^2 \right] > 0 \quad (3)$$

The function Int , plotted in Fig.(1b), implies that for $\nu_{drag}/\nu_{stoch} > 1.04$ there is no steady solution. The non-steady in this region is found to be explosive and a precursor to a chirping solution.

Figure (1a) shows a comparison of the predictions of Eq.(2) with DIII-D and NSTX data. Characteristic values for ν_{stoch} , based on the pitch angle scattering and ν_{drag} were used. As can be seen, the NSTX data points are not in line with predictions of Eq.(2).

This initial comparison of the theory has several shortcomings. The actual theory, discussed in detail Ref.[1, 12] includes contributions from the entire phase space, in (E, P_ϕ, μ) (respectively, energy, angular momentum and magnetic moment) where the physical parameters: ν_{stoch} , ν_{drag} and the particle wave interaction term, $V_{n,j}(E, P_\phi, \mu)$, all have an



appreciable variation in phase space (in particular the pitch angle scattering contribution to ν_{stoch} becomes small when $\mu B/E \ll 1$).

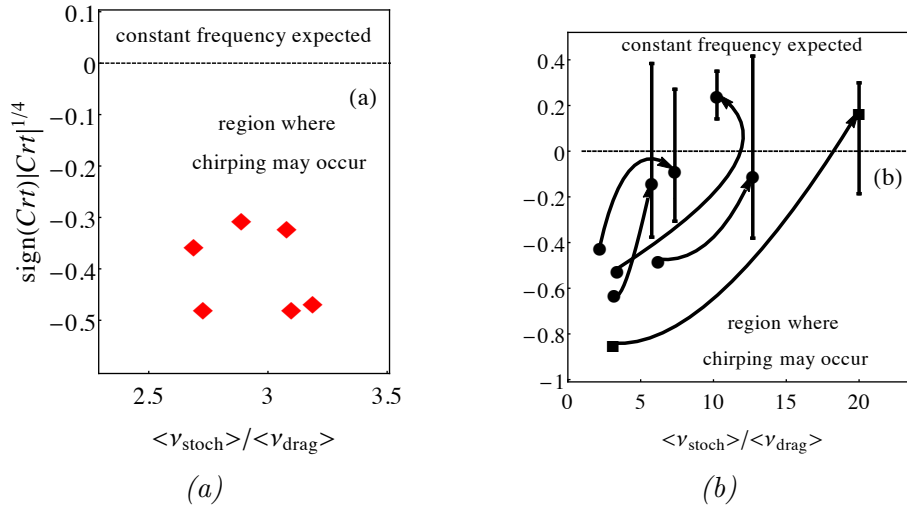
When the physical dependence of phase space parameters is accounted for, the expression for $Crt = Int$ in Eq.(3) is replaced by the phase space averaged expression,

$$\sum_{n,j} \int dE d\mu \frac{2\pi}{\omega_\theta \nu_{stoch,n,j}^4} |V_{n,j}|^4 \left| n^2 \frac{\partial \Omega_{n,j}}{\partial P_\phi} \right|_{E'} \left| Int(E, P_\phi(E, \mu), \mu) \frac{\partial F}{\partial P_\phi} \right|_{E'=E-\omega P_\phi/n} \quad (4)$$

where the integration is over the resonant surfaces $P_\phi(E, \mu)$ defined by:

$\Omega_{n,j}(E, \mu) \equiv n\omega_\phi(E, P_\phi(E, \mu), \mu) + j\omega_\theta(E, P_\phi(E, \mu), \mu) - \omega = 0$ with $\omega_\phi(E, P_\phi(E, \mu), \mu)$ and $\omega_\theta(E, P_\phi(E, \mu), \mu)$ the mean angular toroidal and poloidal frequencies respectively.

This revised equation can be solved, by using for ν_{stoch}^3 the normalized classical pitch angle scattering rate ν_{scatt}^3 , which is the dominant stochastic term in classical theory. We then find that Int can be plotted as a function of ν_{scatt}/ν_{drag} and it has the dependence shown in Fig.(1b). When the phase space dependent ν_{scatt}/ν_{drag} is used for calculating Crt , we find that both the NSTX points and the DIII-D points move to the region where $Crt < 0$ indicating that there should be no steady solutions and implying that in both devices chirping phenomena should be observable. Figure (1b) indicates the source of the qualitative change of predictions. This figure shows that Int achieves much larger magnitudes in the regions where $\nu_{scatt}/\nu_{drag} < 1.04$ than when $\nu_{scatt}/\nu_{drag} > 1.04$, which implies that the contribution from the phase space region where $\mu B/E \ll 1$ can dominate the determination of whether steady state or non-stationary solutions are likely to occur, even when the fraction of particles in this region is relatively small. However, this prediction contrasts with the physical data, which shows that chirping is ubiquitous in NSTX but rarely occurs in DIII-D. To rectify this discrepancy, we propose the inclusion of an additional source for diffusive stochasticity, the ion micro-turbulence generated by the background plasma which can cause spatial diffusion of the energetic ions. Hence, we now add to the expression for ν_{stoch}^3 , the contribution of EP spatial diffusivity due to fast-ion electrostatic micro-turbulence[2], whose scale size is comparable to the ion Larmor radius of the background plasma. Then the determination of this addition to ν_{stoch}^3 is obtained as follows. The TRANSP code [3] is employed to obtain the thermal ion radial thermal conductivity (which is essentially the particle turbulent diffusivity, D_i) based on obtaining the needed thermal conduction coefficient that would match the overall power balance that



is empirically measured. The classical heat thermal conductivity due to collisions is subtracted out and the remaining conductivity is attributed to ion micro-turbulence. Hence, the diffusivity due to background ion turbulence of the background plasma is determined, but we still need to determine the EP diffusivity. This value is estimated by using the scalings found in an electrostatic gyrokinetic simulation [2] model for ITG turbulence, which produced for passing EP particles a diffusivity given by, $D_{EP} \approx 5D_i T_i / E_{EP}$. As in the experiments we analyzed, the EP drive was mostly from the passing particles, this expression is taken for D_{EP} as the base case, with the understanding that in actual experiments there can be considerable variation from this result. To capture this uncertainty, we shall consider that D_{EP} ranges from $2.5D_i T_i / E_{EP} < D_{EP} < 10D_i T_i / E_{EP}$.

Figs.(2a) and (2b) show values of $snCrt1/4 \equiv Crt^{1/4}$ multiplied by the sign of Crt , as a function of the ratio of phase-space averaged stochasticity and drag for Alfvénic modes calculated from the mode structure found from the NOVA[5] code and the particle wave interaction term computed from the NOVAK [5] code. Note that positive value of $snCrt1/4$ indicates the likelihood for steady solutions, while negative values of $snCrt1/4$ indicates the likelihood for chirping. The values of $snCrt1/4$ for the NSTX data is displayed in Fig. (2a) when radial diffusion is neglected. From the TRANSP code it was found the background plasma transport was neo-classical for the experiments analyzed. If the diffusivity from this mechanism is added to the pitch angle scattering contribution to ν_{stoch}^3 , the change in the value of $snCrt1/4$ was found to be imperceptible in the display of Fig.(2a), even though ν_{stoch}^3 increases by a factor ≈ 1.3 . Thus these results indicate that chirping modes are likely to arise in these NSTX experiments as is the case in the actual experiments. The evaluation of $snCrt1/4$ for DIII-D leads to quite different conclusions. The analysis using the TRANSP code indicated that substantial turbulent diffusion is present. Fig.(2b) shows for several DIII-D experiments, the values for $snCrt1/4$ for several values of the spatial diffusion. When the ion turbulent diffusion is neglected (these are the points on the tail of the curvy arrows) and when turbulent radial diffusion is included (these are the points at the heads of the curvy arrows). The limits of the error bars indicate the values of $snCrt1/4$ respectively at half and twice the

base value of the turbulent diffusivity that produces the lower and upper limits of the estimated diffusivity. The experiment shows steady modes in these DIII-D shots. By in large the theoretical curves agree with these observations, especially when the upper limit for $snCrt1/4$ is taken.

We conclude this part of the paper with the following summary:

1. A theoretical criterion for chirping onset of TAE modes in experiment was compared with experimental data in NSTX and DIII-D.
2. Very good correlation was obtained for all the data examined only when the theory incorporated accurate phase space dependence of physical quantities, including: profiles for the mode structure, the pitch angle scattering and the inclusion of energetic particle diffusion due to background turbulence.
3. NSTX data displayed a strong tendency for chirping in agreement with theoretical predictions, as background ion transport, which is low (it is neo-classical) so that classical pitch-angle scattering is the main contributor to the diffusive process.
4. Most DIII-D shots produced steady oscillations during Alfvénic instability. In these shots the background turbulence appeared large enough to prevent chirping from arising.
5. For the rare DIII-D where a chirping response was observed it was found that there was a pronounced reduction in the background ion-turbulence level.
6. This investigation suggest an answer to a previous puzzle for why, when Alfvénic oscillations appear in experimental data in NSTX and DIII-D, chirping Alfvénic modes usually arise in NSTX but only rarely arise in DIII-D.
7. This method of analysis can be applied to other experiments including ITER.

2 Part II: Simulation of the Energetic Particle mode (EPM) and Induced TAE Frequency Avalanche

This section discusses a numerical tokamak model which leads to interesting chirping phenomena with properties similar what has been observed experimentally [7]. For TAE modes the initial trigger frequency lies within the TAE gap and the range of the frequency chirp is limited. In contrast, the EPM modes, whose initial frequency is inside, though at the continuum edge, then rapidly chirps deeper into the continuum to produce a large frequency shift, which in our numerical work is much larger than the gap frequency. Due to the large and fast frequency shift, this phenomenon has been referred to as frequency avalanche [6, 7]. An adiabatic theory for the chirping response is outlined in this paper. This adiabatic theory is found to replicate the evolution of the amplitude and chirping rate vs. frequency shift that were produced by the numerical simulation.

We assume that growth rate of the TAE and EPM modes are slow compared to the mode frequency which then allows for many transit times of the particles around a tokamak before instability causes significant orbit deviation. The nonlinearity is due to the wave-particle interaction that acts on the resonant energetic particles, while the response from the plasma remains linear and the response of the non-resonant energetic particles is assumed small enough to neglect.

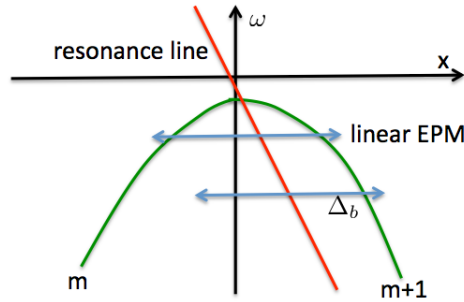


FIG. 3: In a plot of frequency vs. position, the MHD continuum lies on the parabolic-like curve formed by two poloidal harmonics, m and $m + 1$ and a single toroidal harmonic n . The resonant EPs with an orbit width Δ_b , which is depicted by double arrowed horizontal lines, move along the red resonance line. The linear EPM is initially excited in the Alfvén continuum just below the lower tip with the orbit width overlapping both continuum positions. As the mode frequency chirps downward with the resonant particle orbits forming the clump move outward, eventually overlapping just a single TAE resonance position.

Presently our study is confined to large aspect ratio (with $R_0/a \equiv 1/\epsilon \gg 1$, R_0 and a being the major and minor radii) tokamaks with $v_{\parallel}^2/v_{\perp}^2 \gg \epsilon$ so that the modulation of v_{\parallel} along a field line is negligible. As a result of the wave-particle interaction, a resonant particle can cross field lines, while its speed and magnetic moment (μ) do not change. The resulting equations have been simulated for the case where the wave excitation is localized to a single TAE gap region. In this region there is an excitation of the m and $m+1$ poloidal harmonics, and a single toroidal mode number n , such that the gap position is located at $q(r_m) = (m + 1/2)/n$ for relatively low magnetic shear, s ($1 < s^2 < \epsilon$), and the TAE gap frequency $\omega_{TAE} = v_A/(2q(r_m)R_0)$, where v_A is the Alfvén speed at $r = r_m$. The frequency response is chosen to be close to ω_{TAE} and therefore below we use the approximation for time derivatives in the wave equation,

$$\frac{\partial^2}{\partial t^2} \approx \omega_{TAE}^2 \left(1 + \epsilon \left(\omega(t) + v \frac{\partial}{\partial t} \right) \right) + O(\epsilon^2), \quad (5)$$

where $\omega(t)$ is the instantaneous mode frequency relative to the middle of the gap and normalized by the half gap width.

We consider the frequency avalanche case where once there is significant frequency shift, the resonant EPs are locked into the wave structure to enable them to move across field line. During the avalanche, the mode frequency chirps rapidly downward, and the resonant particles move outward so that the resonant particles can only have a single crossing as is shown in Fig.(3).

The dynamics of EPs is governed by the drift kinetic equation,

$$\frac{\partial f}{\partial t} + (\mathbf{v}_{\parallel} + \mathbf{v}_{D0}) \cdot \nabla f + \frac{c}{|\mathbf{B}|} \left[\hat{\mathbf{b}} \times \nabla \left(\frac{\partial \zeta}{\partial t} + v_{\parallel} (\hat{\mathbf{b}} \cdot \nabla) \zeta \right) \right] \cdot \nabla f = 0, \quad (6)$$

where $\mathbf{v}_{D0} = \frac{v_{\parallel}^2 + v_{\perp}^2/2}{\omega_c} (\hat{\mathbf{b}} \times \boldsymbol{\kappa})$ is the unperturbed gradient B and curvature drift velocity of EPs. As the distribution function is solved in time to allow the calculation of the EP

current in the region around $r = r_m$ at each time step. Then one can solve the mode amplitude ψ^+ and ψ^- that satisfy the relations,

$$\left(\omega(t) \pm 1 + i \frac{\partial}{\partial t}\right) \psi^\pm - x \psi^\mp = -C^\mp + \beta_h \int_0^{2\pi} \frac{d\theta}{2\pi} \int_0^{2\pi} \frac{dq}{2\pi} f(q, p, t) e^{-iq} \cdot (e^{-i(l+1)\theta} \pm e^{-i l \theta} - e^{-i(l-1)\theta} \mp e^{-i(l-2)\theta}), \quad (7)$$

where the wave-particle interaction constant is determined from a matching condition,

$$\frac{1}{\pi} \int_{-\infty}^{\infty} \psi^\pm dx = \Delta C^\mp, \quad (8)$$

where Δ is a known complex parameter determined by an outer region solution. The even mode ψ^+ as well as the odd mode ψ^- are driven by the normalized EP's source strength β_h which is proportional to EP's stored energy. Both TAE and EPM modes[13] are found to be unstable in the TAE gap and lower Alfvén continuum, respectively as shown Fig.(4).

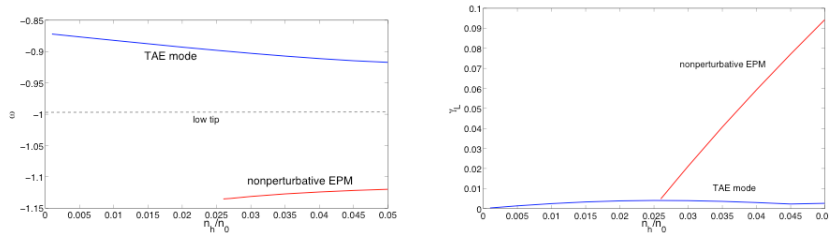


FIG. 4: The linear frequency (left panel) and the growth rate (right panel) of TAE mode in the gap and nonperturbative EPM in the lower continuum, respectively.

A simulation experiment is performed where a source is used to increase the instability drive with time. The resulting evolving spectra is shown in Fig.(5). At first just the perturbative TAE instability is excited, with a limited chirping range. However, as the simulation continues, the EP density builds up, until an EPM is excited in the continuum. The excitation of this mode then leads to a rapid frequency downshift (see Fig.(5)) reminiscent of chirping that occurs in a frequency chirping avalanche that has been reported in experimental observations on NSTX [6, 7].

Physically, this chirping is due to a phase space structure (a clump) moving across field lines, to the outer region of the plasma. When the chirping structure is followed in the frame of the structure, the distribution of the tracked trapped particles in phase space is observed as shown in Fig.(5). This chirping structure is embedded in the same shaped separatrix as is theoretically expected to arise from the observed field amplitude and chirping rate. Thus the shape of the separatrix is consistent with the theoretical prediction.

An analytic theory has been developed, (to be discussed in detail later publication) that reproduces the mode amplitude and chirping rate of the TAE avalanche as is shown in Fig.(6) where the adiabatic approximation i.e. $f = f(J(t))$ is used for the distribution

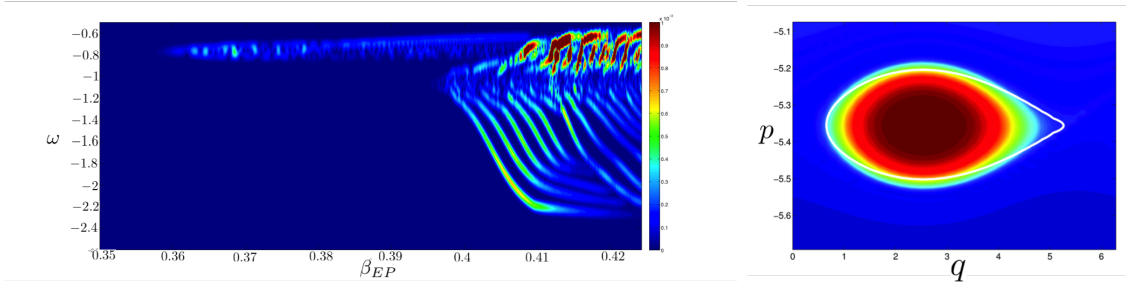


FIG. 5: Evolution of TAE and EPM mode spectrum (left panel) with increasing source strength. The frequency region, $-1 < \omega < 1$, is the TAE gap width. The corresponding trapped particle distribution in phase space (right panel) encompassed by inferred theoretical separatrix shape.

function that determines the energetic particle current. The action J of the wave trapped particle is calculated based on $J = \oint pdq/(2\pi)$ which is assumed to remain invariant during the chirping process in the deep continuum. During the chirp, new particles originally outside the clump will be entrapped by the growing trap wave amplitude and form a new adiabatic invariant surface near the growing updated separatrix.

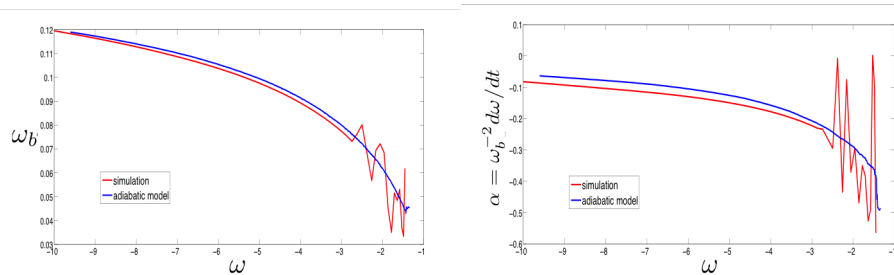


FIG. 6: The bounce frequency (right panel) and chirping rate (left panel) are calculated from the adiabatic theory during the avalanche, which replicate the Vlasov simulation results in the wave frame.

To summarize, a novel numerical method has been developed to study frequency chirping of TAE's and EPM's, where a frequency avalanche develops from the original EPM excitation. After the resonant particles have moved sufficiently outward to have only a single continuum crossing, the newly developed analytic theory predicts the rate and amplitude of frequency avalanche signal as is shown in Fig. (6). The present numerical simulation ignores MHD nonlinearities which are significant. For example, the experimental data [6] for the frequency avalanche shows that the excited mode frequencies produce a rich excitation of frequency harmonics. In future work we intend to further generalize our method. Ultimately the goal is to describe wave-particle resonant excitations in general three dimensional fusion systems whenever the basic unperturbed orbits of the system are integrable.

References

- [1] LILLEY, M.K., et al., “Destabilizing Effect of Dynamical Friction on Fast-Particle-Driven Waves in a Near-Threshold Nonlinear Regime”, *Phys.Rev.Lett.* 102(2009) 195003.
- [2] ZHANG, W., et al., “Transport of Energetic Particles by Microturbulence in Magnetized Plasmas”, *Phys. Rev.Lett.* 101(2008) 095001.
- [3] HAWRYLUK, R.J., et al., “in Physics of Plasmas Close to Thermonuclear Conditions Vol.1”, CEC, Brussels(1980).
- [4] GHANTOUS, K., et al., “1.5D quasilinear model and its application on beams interacting with Alfvén eigenmodes in DIII-D”, *Phys.Plasma* 19(2012) 092511.
- [5] GORELENKOV, N.N., et al., “Fast particle finite orbit width and Larmor radius effects on low-n toroidicity induced Alfvén eigenmode excitation”, *Phys.Plasmas* 6(1999) 2802.
- [6] PODESTA, M., et al., “Study of chirping toroidicity-induced Alfvén eigenmodes in the National Spherical Torus Experiment”, *Nucl. Fusion* 52(2012) 094001.
- [7] FREDRICKSON, E.D., et al., “Parametric dependence of fast-ion transport events on the National Spherical Torus Experiment”, *Nucl.Fusion* 54(2014) 093007.
- [8] SYKES, A., et al., “First results from MAST”, *Nucl. Fusion* 41(2001) 1423.
- [9] BERK, H.L., et al., “Nonlinear Dynamics of a Driven Mode near Marginal Stability”, *Phys.Rev.Lett.* 76(1996) 1256.
- [10] BERK, H.L., et al., “Spontaneous hole-clump pair creation in weakly unstable plasmas”, *Phys.Lett.* 234(1997) 213.
- [11] BREIZMAN B.N., et al., “Critical nonlinear phenomena for kinetic instabilities near threshold”, *Phys.Plasmas* 4(1997) 1559.
- [12] BERK, H.L., et al., “Nonlinear theory of kinetic instabilities near threshold”, *Plasma Phys. Rep.* 23(1997) 778.
- [13] CHEN, L., “Theory of magnetohydrodynamic instabilities excited by energetic particles in tokamaks”, *Phys. Plasmas* 1(1994) 1519.